Coherent Sources for Mid-Infrared Laser Spectroscopy (Invited)

Pavel Honzatko, Yauhen Baravets, Shyamal Mondal, Pavel Peterka, Filip Todorov

Institute of Photonics and Electronics, CAS, Prague, Czech Republic

1. INTRODUCTION

Keywords: Laser absorption spectroscopy, TDLAS, CEAS, CRDS, WMS, FMS, DCS, trace gas analysis, single-frequency lasers, fiber laser, fiber amplifier

Mid-infrared laser absorption spectroscopy (LAS) is useful for molecular trace gas concentration measurements in gas mixtures. While the gas chromatography-mass spectrometry is still the gold standard in gas analysis, LAS offers several advantages. It takes tens of minutes for a gas mixture to be separated in the capillary column precluding gas chromatography from real-time control of industrial processes, while LAS can measure the concentration of gas species in seconds. LAS can be used in a wide range of applications such as gas quality screening for regulation, metering and custody transfer,[1] purging gas pipes to avoid explosions,[1] monitoring combustion processes,[2] detection and quantification of gas leaks,[3] by-products monitoring to provide feedback for the real-time control of processes in petrochemical industry,[4] real-time control of inductively coupled plasma etch reactors,[5,6] and medical diagnostics by means of time-resolved volatile organic compound (VOC) analysis in exhaled breath.[7] Apart from the concentration, it also permits us to determine the temperature, pressure, velocity and mass flux of the gas under observation. The selectivity and sensitivity of LAS is linked to a very high spectral resolution given by the linewidth of single-frequency lasers. Measurements are performed at reduced pressure where the collisional and Doppler broadenings are balanced. The sensitivity can be increased to ppb and sometimes to ppt ranges by increasing the interaction length in multi-pass gas cells or resonators and also by adopting modulation techniques.[8]

2. OVERVIEW OF VARIETIES OF LASER ABSORPTION SPECTROSCOPY

Many varieties of LAS have been developed over years aimed at improving of optical detection and increasing the interaction length. The various LAS techniques are reviewed below.

2.1 Tunable diode laser absorption spectroscopy

Tunable diode laser absorption spectroscopy (TDLAS) performs scanning over one or several absorption lines of the gaseous mixture using a narrowband laser line. The resolution of the technique is given by the laser linewidth. Single-frequency lasers operated at a single longitudinal/transversal mode should be used. The usefulness of tunable single-frequency laser diodes for high-resolution absorption spectroscopy was recognized by E.D. Hinkley[9,10] of MIT Lincoln Laboratory. TDLAS scheme is shown in Fig. 1a. Saw-tooth voltage drives the injection current of a laser diode or a Peltier thermoelectric cooler to scan the laser wavelength over a narrow spectral range. The laser light interacts with the analysed gas in a gas cell and the output signal is detected by a photodetector. The signal from the photodetector is sampled and digitized by a high-resolution A/D converter and finally processed in a computer. The molecular absorption line manifests itself as a decrease in the detector photocurrent, as can be seen in Fig. 1b. A small decrease in a large signal has to be measured if very small concentrations of molecules are analysed. Such detection tasks are usually solved by the lock-in detection technique.

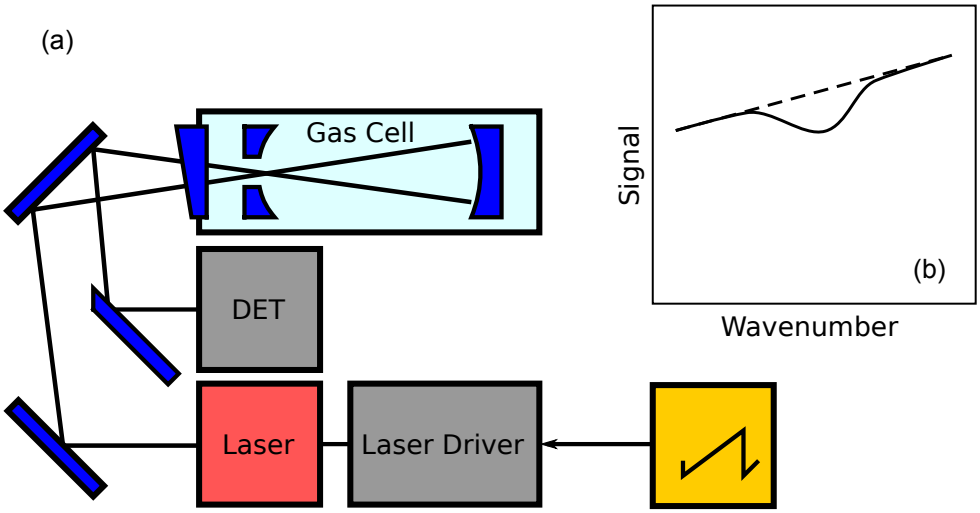

Figure 1. (a) Principal scheme of TDLAS. (b) measured signal across the molecular absorption line.

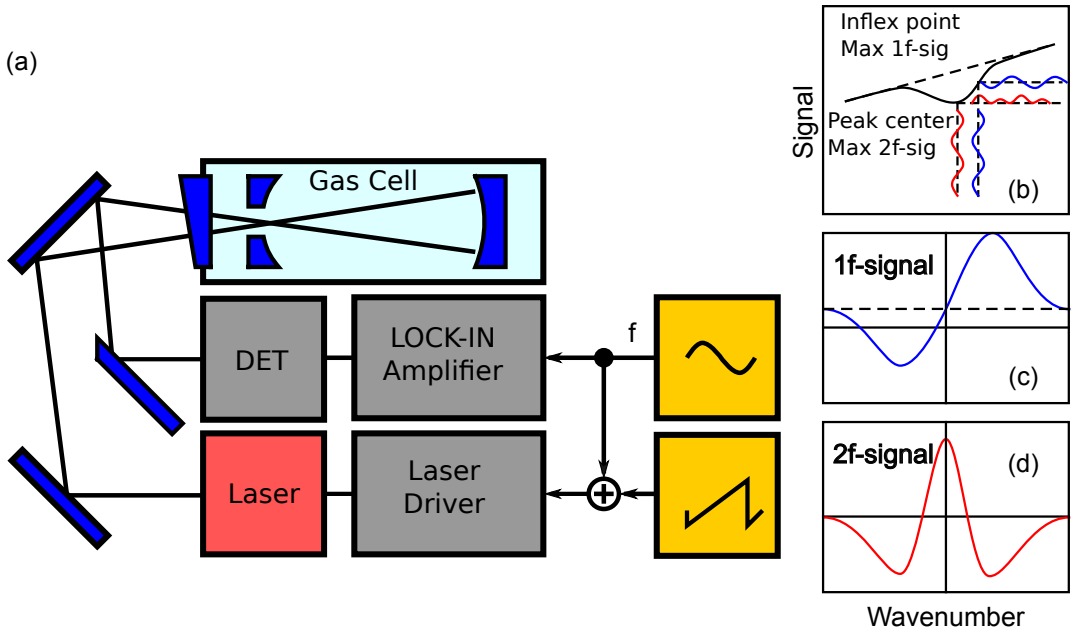

Figure 2. (a) Principal scheme of WMS, eventually FMS technique. (b) Conversion of wavelength modulated signal into amplitude modulated signal. Dependence of the (c) first harmonic and (d) second harmonic of modulation signal on the wavenumber.

2.2 Wavelength modulation spectroscopy

Wavelength modulation spectroscopy (WMS) is a typical example of the lock-in detection technique for the detection of small changes in large signals. The principal scheme of the WMS technique is shown in Fig. 2a, where a sine-generator operating at frequency f and lock-in amplifier are included. The sinusoidal signal is superimposed on the ramp signal and causes the laser wavelength to vary sinusoidally while the laser scans across the molecular transition. The range of these oscillations should be comparable to the molecular transition width. The harmonic signal is separated by using a lock-in amplifier, which greatly reduces the influence of laser and electronic noise by filtering the components of the detector signal that are close to the corresponding harmonics. First harmonic of the modulation signal (1f-signal) is usually non-zero even outside the molecular transition due to the residual amplitude modulation (RAM) of the modulated laser diode. The second harmonic of the modulation signal is usually employed to eliminate this unwanted background with an additional advantage

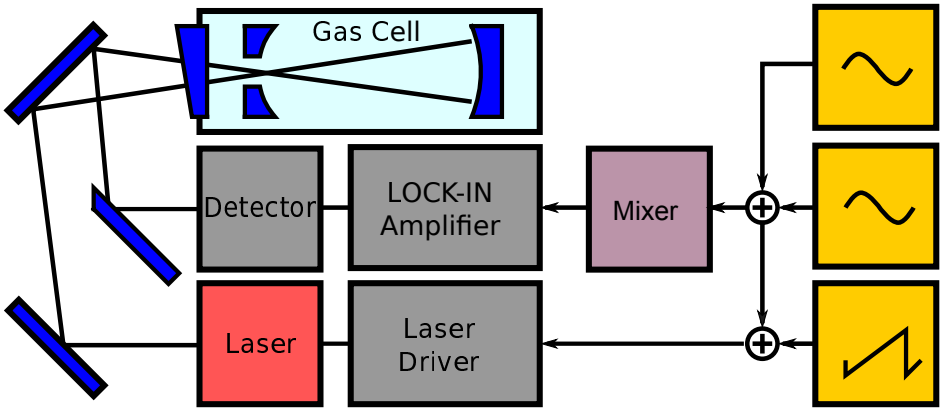

Figure 3. Principal scheme of 2T-FMS technique.

that the 2f-signal peak corresponds to the absorption peak. A reference gas cell with a known concentration of the analysed gas is often used to calibrate the WMS system, which, however, increases the complexity of the system. Several techniques have been developed that avoid the necessity of emplying the reference cell using the 1f-signal,[11] 2f-signal,[12,13] or 2f-signal normalized to the 1f-signal (2f-/1f-signal).[14] The driving signal is often sampled and digitized together with the detected signal and phase-insensitive software lock-in is used instead of a hardware lock-in amplifier.[14]

2.3 Frequency modulation spectroscopy

Frequency modulation spectroscopy (FMS) is another example of the lock-in detection technique for the detection of small changes in large signals. It was first proposed and demonstrated by Bjorklund.[15] The measurement setup is the same as for WMS (Fig. 2). The technique differs from WMS in that it uses high modulation frequencies and a modulation index close to 1, which is much smaller than that used in WMS. The modulation frequency should be higher than the width of the probed absorption feature. The technique is particularly suitable if lasers with high excess noise are used. The laser excess noise has 1/f character and thus decreases with increasing frequency. Modulation of the laser at a sufficiently high frequency combined with lock-in detection allows us to eliminate this source of noise. A disadvantage of the technique is the necessity of using a high-bandwidth detector and lock-in amplifier. The FMS is the preferred technique if lead-salt laser diodes with high laser excess noise are used. FMS and WMS seem to be comparable for the state-of-the-art spectroscopy systems based on room-temperature distributed feedback (DFB) or extended cavity (EC) diode lasers.[1]

2.4 Two-tone frequency modulated spectroscopy

Two-tone frequency modulated spectroscopy (2T-FMS) was introduced by Janik *et al.* to overcome the necessity using wide-bandwidth mid-infrared detectors and lock-in amplifiers in FMS.[16] The principal scheme of the technique is shown in Fig. 3. Two sine-wave generators with slightly different frequencies are used. The frequencies of the generators should be comparable to the width of the sensed molecular line while their difference should lay within the bandwidth of the detection system. The signals are mixed together to get the difference frequency signal that serves as a reference for the lock-in amplifier. They are also combined and used to drive the electro-optical phase modulator or superimposed on the ramp signal and employed for direct modulation of the laser diode.

2.5 Cavity enhanced techniques

Resonant cavities can provide very large path length enhancement, in the order of the finesse of the cavity,[1] which can be as high as 10^4 to 10^5. A breakthrough in the resonator finesse in the near-infrared as well as mid-infrared spectral range has been recently achieved with supermirrors prepared by ion-beam sputtering on super-polished substrates and supermirrors based on substrate-transferred crystalline coatings.[17] Amorphous coatings consisting of alternating thin layers of high-index metal oxides like tantala Ta_2O_5 and low-index silica

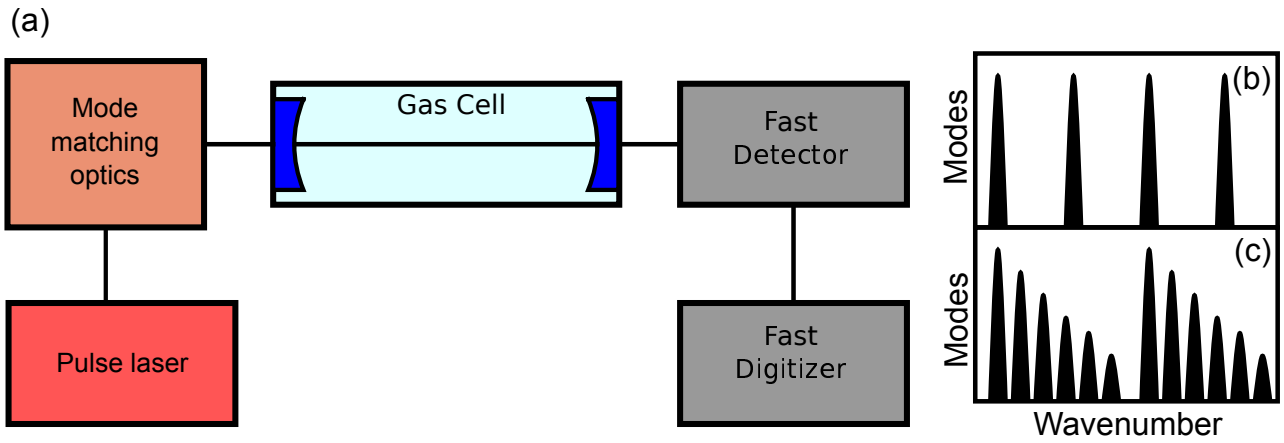

Figure 4. (a) Principal scheme of CRDS technique. (b) Mode structure of confocal, and (c) stable (non-confocal) resonator.

SiO_2 suffer from significant absorption at wavelengths beyond $2\,\mu$m and excess Brownian noise, related to displacement fluctuations of the mirror surface arising from thermally driven mechanical modes. This problem is solved by using substrate-transferred crystalline coatings.[17] The substrate-transferred coating procedure entails separating the epitaxial multilayer from its original growth wafer and directly bonding it without the use of adhesives or intermediate films to the chosen host substrate. Absorption and scattering in the coatings can be lower than 1 ppm and 5 ppm at 1064 nm, respectively.[18] The loss of supermirrors achieves hundreds of ppm in the mid-infrared.[17] With both these techniques, the cavity finesse can reach a value as high as 300,000 in the near infrared. The main problem with resonant cavities is that a high-finesse cavity has narrow cavity modes, often in the kilohertz range. Therefore, it is difficult to couple laser light into high-finesse cavities effectively.

2.5.1 Cavity ring-down spectroscopy

In cavity ring-down spectroscopy (CRDS), the problem with coupling laser light into narrowband cavity modes is circumvented by injecting a short light pulse in the cavity. The injected pulse bounces between the two dielectric cavity mirrors, each reflection resulting in a small portion of the pulse being emitted from the cavity. The transmitted pulses decay exponentially due to finite reflectivity of the mirrors, their imperfections, and additional loss such as resonant molecular absorption. The rate of the decay is measured rather than the magnitude of absorption, which makes this technique insensitive to light source intensity fluctuations. Extremely long effective path lengths (many kilometers) can be obtained in this way. The principal scheme is shown in Fig. 4. A laser pulse with a duration typically from 1 to 20 ns and relatively high energy ($10\,\mu$J – 1 mJ) is coupled through the mode-matching optics into the cavity and the ring-down transient is recorded with an MCT detector. A two-lens telescope combined with a pinhole is used for transversal mode-matching. The decay transient is recorded with a fast high-resolution (at least 10-bit) analog-to-digital converter or oscilloscope for three or four decay times of the empty cavity. In the original formulation by O'Keefe and Deacon,[19] the a broadband excitation laser with a short coherence length was used, which limits the resolution of the technique. Meijer et al. proposed using a stable (non-confocal) resonator with a dense transverse cavity mode spectrum to increase the pulse coupling efficiency and spectral resolution of the technique.[20]

2.5.2 Integrated cavity output spectroscopy

Integrated cavity output spectroscopy (ICOS) was introduced by O'Keefe as the next generation of cavity-enhanced techniques.[21] The principal scheme is shown in Fig. 5. A single-frequency CW laser is used instead of a pulse laser to achieve high resolution of spectral lines. One of the cavity mirrors is dithered faster than the cavity mode builds-up to wash out the cavity mode structure preventing a significant energy build-up in any particular mode. A signal output involving integration over a large number of partly excited cavity modes is measured, enabling the use of a slow detector and digitizer while still retaining the long path lengths of high-finesse cavities. The necessary detection bandwidth for ICOS is in a range of 10 – 100 kHz compared to 1 MHz for the CRDS.

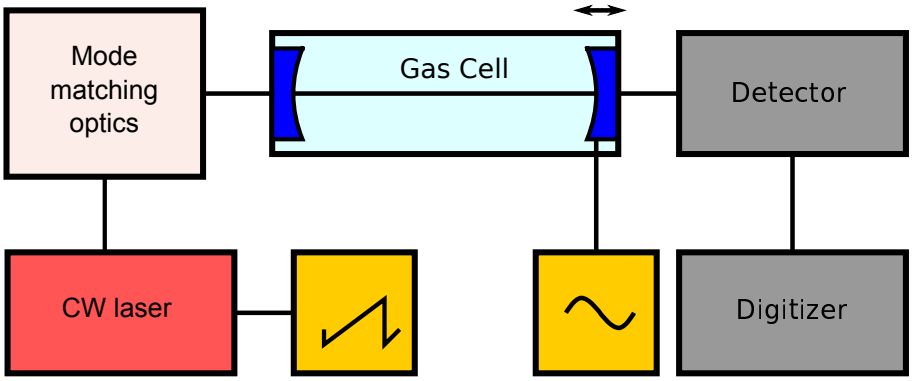

Figure 5. Principal scheme of ICOS, eventually CEAS technique.

Alrernatively, scanning single-frequency laser is employed to couple light into a stable (non-confocal) resonator.[22] Many modes of the quasicontinuum mode structure of the stable resonator are evenly excited by rapidly scanning the laser, while the signal leaking from the cavity is integrated over time by a slow detector and then plotted with the wavelength of the laser.

2.5.3 Off-axis integrated cavity output spectroscopy

The noise equivalent absorption in ICOS is limited by imperfect averaging of the cavity response function, which manifests itself as noise in the measured absorption spectra. The off-axis alignment of the cavity axis with respect to laser beam was proposed to increase the cavity mode density and eliminate the source of noise.[23] The optical path is increased in a multi-pass arrangement before the reentrant condition is achieved, while the free spectral range (FSR) of the cavity and mode-width are decreased, correspondingly. The FSR to mode-width ratio given by the cavity finesse remains unchanged. The mode-width ultimately reaches a lower limit determined primarily by mechanical fluctuations in the system and imperfections in the mirror surfaces. The mode structure is effectively suppressed at this point and the cavity transmission becomes independent of frequency, being determined solely by the round-trip cavity loss. In contrast to multi-pass gas cells, light is not extracted from the cavity by means of a hole in the mirror, which simplifies the alignment significantly. A side effect of the off-axis alignment is the suppression of back reflections which could otherwise destabilize the laser. The main drawback of this approach is significantly lower power transmission through the cavity compared to resonant-coupling methods. Another drawback is a large transverse dimension of the cavity since the off-axis integrated cavity output spectroscopy (OA-ICOS) performance depends on the ability to excite transverse cavity modes of very high order, whose superposition gives rise to folded quasi-periodic trajectories. This results in large cavity volumes and correspondingly high sample flows.[24]

2.5.4 Optical feedback cavity enhanced absorption spectroscopy

The optical feedback cavity enhanced absorption spectroscopy (OF-CEAS) technique exploits the resonant optical feedback coming back from a high-finesse cavity into the laser source. The optical feedback is used for injection-locking the laser to the cavity resonance, which results in a high efficiency of light coupling and low transmission noise for the cavity. Moreover, high intracavity field enables the sub-Doppler saturation spectroscopy to be performed. A V-shape cavity was used by Romanini *et al.* to optically feedback a small portion of the intracavity field while the direct back reflection from cavity mirror is avoided (Fig. 6). The optical feedback helps narrow the laser line down to a few kilohertz. High path length enhancement combined with excellent noise properties of DFB-QCL allows scaling the sensitivity of the technique to ppt levels.[25]

2.5.5 Noise-immune cavity-enhanced optical heterodyne molecular spectroscopy

Noise-immune cavity-enhanced optical heterodyne molecular spectroscopy (NICE-OHMS) represents CEAS technique with the laser line tightly locked to a cavity mode. Frequency modulation is used to achieve shot-noise limited recovery. The modulation frequency should be precisely equal to the FSR of the cavity. The carrier and the sidebands then propagate with the same complex transmission coefficient and no conversion of frequency

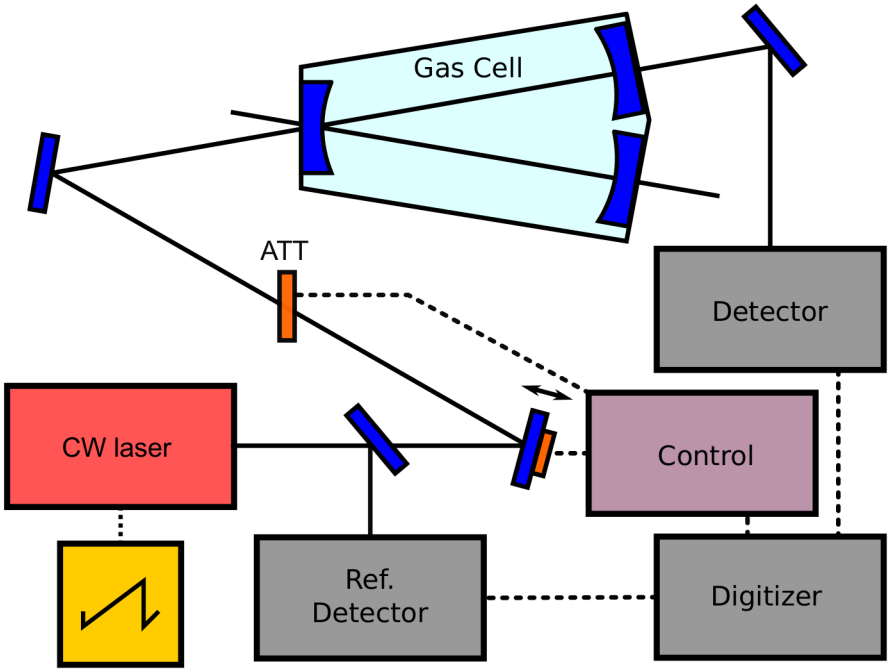

Figure 6. Principal scheme of OF-CEAS technique.

.

modulation to amplitude modulation occurs. The central cavity mode will be frequency-pulled due to an additional phase shift caused by the molecular dispersion in the presence of molecules with the resonant transition. The phase-sensitive detector, responding to the transmitted light, thus generates a dispersion signal at the rf-beat frequency.[26] The cavity is scanned/dithered with a small amplitude to probe the molecular transition shape and low-frequency modulation is applied to the laser signal to lock the laser to the cavity mode. The scheme of the NICE-OHMS technique is shown in Fig. 7.

2.5.6 Dual-comb spectroscopy

Dual-comb spectroscopy (DCS) was proposed by Schiller in 2002.[27] The DCS concept is illustrated in Fig. 8. A femtosecond mode-locked laser features a broadband spectrum consisting of large number of modes separated by the repetition frequency, which is called the frequency comb. Two combs, slightly differing in the repetition frequency, are mixed and detected by a photodiode. Each pair of comb lines yields an rf heterodyne signal at a unique frequency. Either one (dispersive technique) or both (absorption technique) combs are passed through the sample and the absorption or phase shift is encoded onto the corresponding beat signal.[28] DCS maps the optical spectrum of width $\Delta\nu$ onto the rf-spectrum of width $\Delta\nu/m$, where $m = \bar{f}_r/\Delta_r$ is the compression factor, $\bar{f}_r = (f_{r1} + f_{r2})/2$ is the average comb repetition frequency, $\Delta_r = f_{r2} - f_{r1}$ is the repetition frequency difference. The repetition frequency difference should be small

$$\Delta_r < \frac{\bar{f}_r^2}{2\Delta\nu}$$

to allow for unambiguous spectral mapping. The main advantage of the technique is the absence of the tuning process and that the whole spectrum is acquired relatively quickly in a time period $1/\Delta_r$.

2.6 Comparison of LAS techniques

We have provided an extensive, although not exhaustive review of various LAS techniques. Generally, the techniques follow two approaches. The first approach tries to achieve the shot-noise limited signal recovery through the use of an appropriate modulation technique shifting the detection from the baseband frequencies

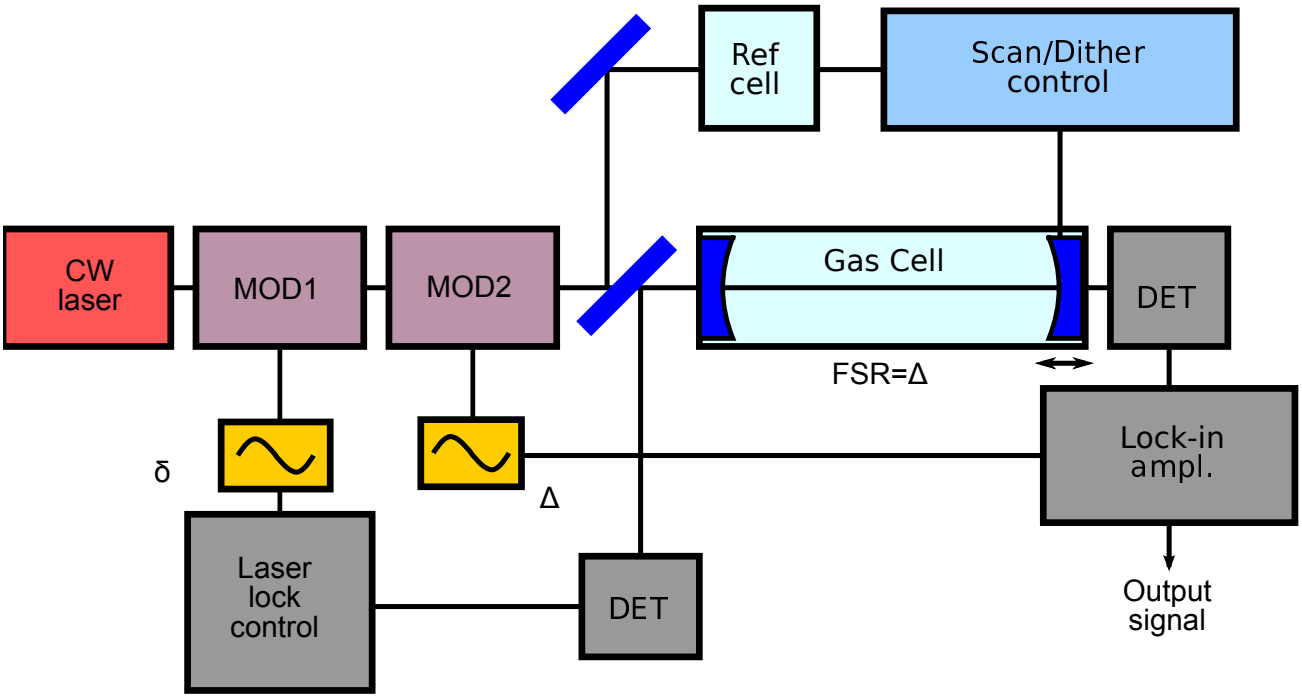

Figure 7. Principal scheme of NICE-OHMS technique.

.

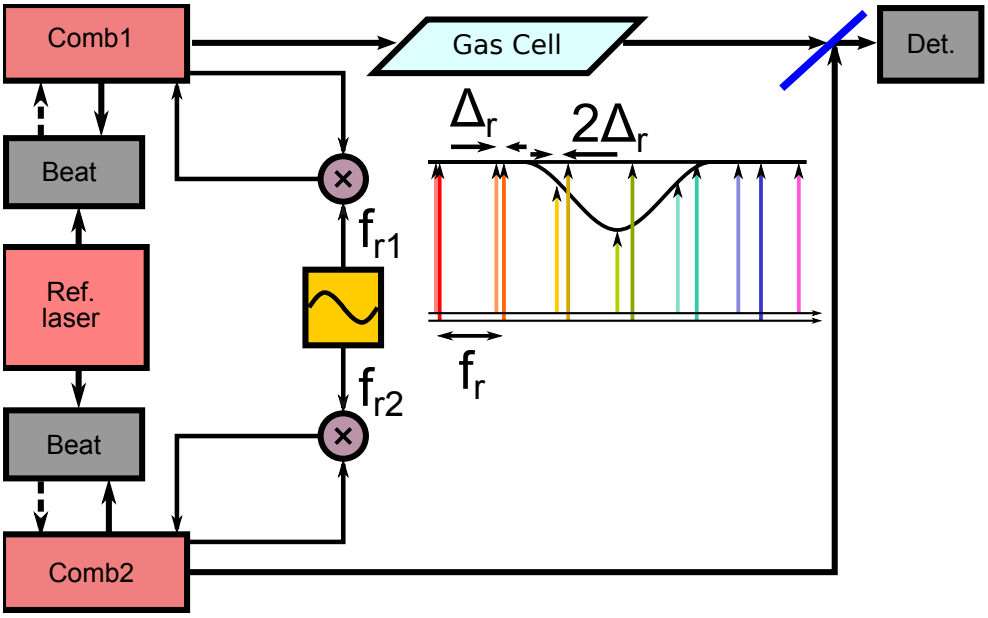

Figure 8. Principal scheme of DCS technique

.

to frequencies where various kinds of noise are low. In the second approach, the absorption itself is increased in a high-finesse cavity. It appears that WMS, FMS, 2T-FMS techniques all allow us to achieve the shot-noise limited operation if fed from low-noise lasers.[1] The spectral resolution of CRDS is principally limited due to finite spectral bandwidths of optical pulses. This is not the case for DCS, where the pulse spectra are broadband and the individual spectral lines are well defined so that beating of two close spectral lines can be recorded. The spectrum is sampled in discrete points separated by tens of megahertz. Cavity-enhanced techniques usually do not attain the shot-noise limit. Nevertheless, their large long interaction length makes them extremely sensitive to small concentrations of trace gases so that they can compete with gas chromatography techniques in sensitivity. Moreover, their response is much faster. OF-CEAS and NICE-OHMS belong to the most sensitive techniques.

3. COHERENT SOURCES FOR LAS

3.1 Requirements

All the methods we have described except for the CRDS and DCS rely on single-frequency CW lasers. In the following we will formulate basic requirements on CW coherent sources for LAS.

3.1.1 Power

First we relate the noise equivalent absorption and power of the signal. The signal power at the output of a multi-pass cell filled with a gas mixture is given by Lambert-Beer law as

$$P_g = P_{in} T_{gc} \exp[-\alpha(\tilde{\nu}) L], \tag{1}$$

where P_{in} is the power at the input of the gas cell, T_{gc} is transmission of the empty gas cell, $\alpha(\tilde{\nu})$ is the spectral absorption coefficient at wavenumber $\tilde{\nu}$. The signal power of the empty cell is $P_0 = P_{in} T_{gc}$. We can therefore write

$$\alpha(\tilde{\nu}) L = \frac{P_g - P_0}{P_0} \tag{2}$$

in the limit of small absorption, $\alpha L \ll 1$. The power at the gas cell output is measured by a photodetector. The detector photocurrent is given by the responsivity of the detector, $i = \mathcal{R} P$. The measurable change in the numerator of the equation (2) is obviously limited by the photocurrent fluctuations. The minimum measurable $\alpha_{min} L$ is called noise-equivalent absorption, NEA,

$$NEA = \alpha_{min}(\tilde{\nu}) L = \frac{\langle \delta i_0 \rangle}{i_0} = SNR^{-1}, \tag{3}$$

and is equal to the inverse of the signal-to-noise ratio, which can be written as

$$SNR = \sqrt{\frac{\langle \delta i_0^2 \rangle}{\langle \delta i_{TN}^2 \rangle + \langle \delta i_{SN}^2 \rangle + \langle \delta i_{1/f}^2 \rangle}}, \tag{4}$$

where $\langle \delta i_{TN}^2 \rangle$ is the detector thermal noise, $\langle \delta i_{SN}^2 \rangle$ is the shot noise, and $\langle \delta i_{1/f}^2 \rangle$ is the laser excess noise.[29] The thermal noise is given by the equivalent resistance of the detection system and bandwidth of the detector and doesn't depend on the photocurrent. The laser excess noise is frequency dependent and can be neglected if the system is operated at a sufficiently high frequency. The shot-noise is given by Poissonian character of light and is proportional to the mean photocurrent i_0 and detection bandwidth B,

$$\langle \delta i_{SN}^2 \rangle = 2 e i_0 B. \tag{5}$$

This noise source becomes dominant when the mean photocurrent is sufficiently high. The regime of this type is called shot-noise limited and

$$NEA = \sqrt{\frac{2eB}{i_0}} = \sqrt{\frac{2eB}{\mathcal{R} P}}. \tag{6}$$

The NEA is slightly impaired when FM is used to perform the detection at high frequencies to get rid of the laser excess noise

$$NEA = \sqrt{\frac{2eB}{\mathcal{R}P}} \frac{\sqrt{2}}{J_0(\beta)J_1(\beta)} = \sqrt{\frac{2eB}{\mathcal{R}P}}\Pi, \tag{7}$$

where $J_0(\beta)$ and $J_1(\beta)$ are Bessel functions of zeroth and first orders, respectively, and β is the modulation index.[26] The smallest penalty $\Pi \approx 4.16$ is achieved for $\beta \approx 1.1$. The penalty is reasonably small if we take into account that at the modulation frequency the laser excess noise can be from two to four orders of magnitude lower.[1] Now we can estimate that the NEA value can be as low as 3×10^{-8} for a signal power of 1 mW, photodetector responsivity of 1 A/W, and integration time equal to 1 s, corresponding to bandwidth $B = 1/2\pi$ Hz. For other NEA and B, the required power scales in accordance with equation (7).

3.1.2 Linewidth

The laser linewidth determining the resolution of the LAS technique should be much narrower than the width of the measured molecule absorption line. The molecular absorption linewidth is influenced by Doppler and collisional broadening. Doppler broadening is given by the distribution of molecular velocities and leads to a Gaussian line shape. Its FWHM Γ_G depends on the absolute temperature T and mass of the molecule m as

$$\Gamma_G = 2\nu\sqrt{\frac{2\ln 2 k_B T}{mc^2}}, \tag{8}$$

where k_B is the Boltzmann constant. Collisional broadening is caused by molecular collisions which decrease upper state lifetimes. It leads to a Lorentz line shape whose FWHM Γ_L depends on the gas pressure p as

$$\Gamma_L = 2p[\gamma_{air}(1 - c_v) + \gamma_{mol}c_v], \tag{9}$$

where γ_{air} and γ_{mol} are the air-broadened and self-broadened half widths, the values of which can be found, for example, in HITRAN database, and c_v is the volume concentration of the measured gas. The resulting absorption line shape is known as the Voigt profile and is given by the convolution of Lorentzian and Gaussian functions.

The general strategy at high-resolution spectroscopy is to decrease the pressure to a point where collisional and Doppler broadening are equal. Ethane, C_2H_6, with a molar mass of 30.069 g/mol, can be taken as an example. Its molecular mass is $5 \times 10^{-26} kg$. Doppler broadening of lines around 3000 cm^{-1} is found to be 200 MHz at room temperature using the Eq. (8). Therefore, the laser line should be much narrower than this value. The situation is different for OF-CEAS and NICE-OHMS, where the laser line is locked to a mode of a high-finesse cavity. Then the laser linewidth ought to be much smaller than the cavity mode width, which could be as small as 10 kHz. Such a narrow laser linewidth combined with an exceptional sensitivity of cavity-enhanced techniques and strong intracavity field can be used for Doppler-free measurements using the saturation absorption spectroscopy, allowing the resolution of lines as narrow as 100 kHz.[26] These measurements should be performed at much lower pressures, in mtorr, instead of torr range.

The linewidths of single-frequency diode lasers are usually hundreds of kHz or more. This linewidths can be decreased by an electronic feedback loop,[30] optical feedback, or self-injection.[31] The techniques of noise reduction matured for the near-infrared but are still waiting to be transferred and demonstrated for the mid-infrared. The linewidths of single-frequency fiber lasers could be below 1 kHz. Parametric nonlinear optical processes are employed to convert the laser light into the mid-infrared spectral range.

3.1.3 Relative intensity noise

Relative intensity noise (RIN) is defined as a ratio of the mean-square optical power noise to the square of the average optical power,

$$RIN(f) = \frac{SPD(f)}{P^2}, \tag{10}$$

where $SPD(f)$ is the (single-sided) spectral power density at frequency f. RIN results from beating between the spontaneous and stimulated emission, relaxation oscillations, carrier recombination processes in diode lasers, and electronic noise from laser drivers. Generally, diode lasers exhibit relaxation oscillations at much higher frequencies ($\approx$ 1 GHz) than fiber lasers ($\approx$ 100 kHz). The RIN peak related to relaxation oscillations is reduced and shifted towards higher frequencies for stronger pumping in both types of lasers.[32]

3.2 Laser diodes

Laser diodes are sources of first choice wherever they are applicable. They are rugged, small and easy to operate. The output power is usually in a range of $1 - 10\,\mathrm{mW}$. Their output beam is usually highly astigmatic and needs special collimating optics. The single frequency regime tunable in a narrow spectral range through temperature or current control is achieved by means of distributed feedback structures. A broad-band tunability can be obtained in extended-cavity lasers. Commercial extended-cavity lasers are achieving impressive tunability in the near-infrared spectral range. Lasers with mode-hop-free tuning over more than 10% of their center frequency (200 nm around 1540 nm center frequency) are available. Their linewidths are usually hundreds of kHz and can be further decreased by optical fiber interferometers and appropriate electronic control by several orders of magnitude.[30] The laser diode sources for the mid-infrared still lack this state of maturity. III-V group semiconductor laser diodes based on antimony are used up to the wavelength of $3.7\,\mu\mathrm{m}$. IV-VI group semiconductors are used for wavelengths $3 - 30\,\mu\mathrm{m}$. Interband cascade lasers (ICL) belong to emerging technologies for wavelengths $3 - 6\,\mu\mathrm{m}$, while quantum cascade lasers (QCL) attract more and more interest for wavelengths above $3.5\,\mu\mathrm{m}$. A pulse QCL was first demonstrated in 1994,[33] and first room-temperature operation of CW QCL in 2002.[34] ICL was presented by Rui Q. Yang in 1995,[35] and ICL lasing in the CW mode at room temperature was first demonstrated in 2008.[36] The tunability of DFB ICL and DFB QCL is typically between 0.05% and 1% of the center wavelength. The tunability of the most broadband, bound-to-continuum quantum cascade extended-cavity lasers (QC-ECL), reaches 10%-15% of the center frequency, while the mod-hop-free tuning range of commercial QC-ECLs reaches $60\,\mathrm{cm}^{-1}$. Their linewidth is typically several MHz. RIN decreases with increasing power.

3.3 Optical parametric oscillators

Single-frequency parametric nonlinear optical processes allow us to achieve the widest tuning ranges in the mid-infrared. Optical parametric oscillators (OPO) are based on parametric generation of the signal and idler at the expense of the pump power. High conversion efficiency can be achieved thanks to the presence of a cavity resonant at the signal frequency. Their threshold power can be decreased by two orders of magnitude in doubly resonant OPO, where cavity is resonant both for the signal and idler, or pump-resonant (pump-enhanced) OPO, where the cavity is resonant for both the signal and pump. The key enabling technologies for broadband, continuously tunable OPO are broadband dielectric mirrors, high-power widely tunable single-frequency pump lasers with diffraction-limited beams, advanced frequency stabilization techniques, and periodically poled crystals.[37] Periodically poled crystal allow us to achieve the phase synchronism in spectral regions where this would be otherwise impossible. Periodically poled oxide crystals can cover a mid-infrared spectral region of $3 - 4.5\,\mu\mathrm{m}$, while orientation-patterned crystals like GaAs can extend this spectral range up to $16\,\mu\mathrm{m}$ in the far-infrared. ZGP crystals pumped at wavelengths longer than $2.1\,\mu\mathrm{m}$ can be alternatively used for the generation of radiation up to $12\,\mu\mathrm{m}$. The frequency of single-frequency singly resonant OPO is usually stabilized by means of an intracavity elalon. Mode-hop-free tuning over a large spectral range is still to be demonstrated.

3.4 Difference frequency generators

Difference frequency generation (DFG) is another parametric nonlinear optical process used to achieve broad mode-hop-free tuning. Coherent sources based on difference frequency mixing of signals from near-infrared, fiber-coupled lasers have several distinctive advantages compared to other laser sources. Single-mode single-frequency fiber sources generate diffraction-limited beams and exhibit very low laser excess noise. Near-infrared, fiber-coupled extended cavity laser diodes have a mod-hop-free tuning range up to 12% of the center frequency and feature linewidths on the order of hundreds of kHz. These linewidths can be further decreased using appropriate noise-reduction techniques due to the availability of low-loss optical fiber interferometers.[30,38,39] Fiber-pigtailed phase modulators allow achieving phase modulation with small RAM. Fiber wavelength-division multiplexers simplify the alignment of the source.[40,41] A single-mode, diffraction-limited beam is well suited for propagation over long distances in multi-pass gas cells and cavities operated at single transversal mode. The line shape of the difference frequency signal is given by the convolution of the line shapes of two interacting fundamental laser signals and line widths ranging from kilohertz to megahertz are then achievable. The main disadvantage of difference frequency mixing is its low conversion efficiency.

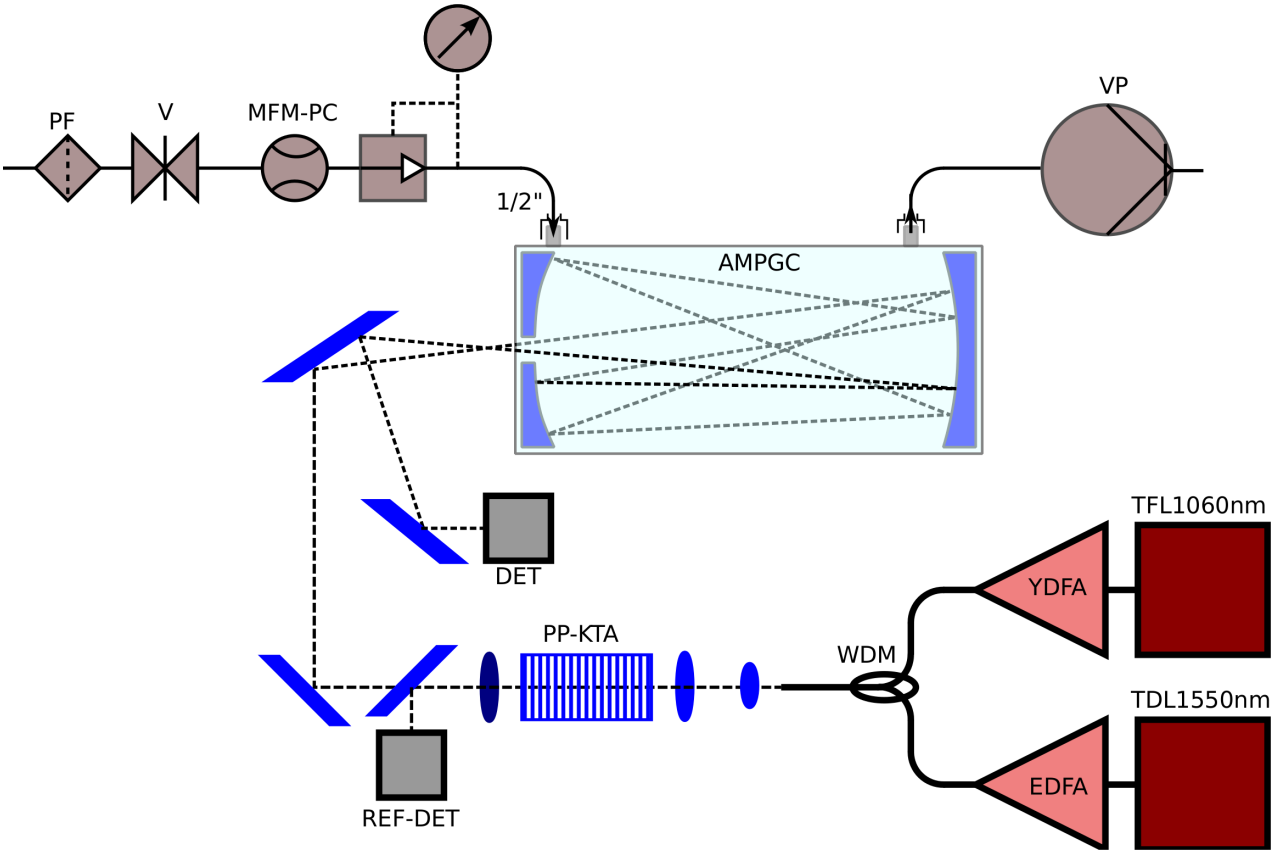

Figure 9. Laser absorption spectroscopy system.

4. LASER ABSORPTION SPECTROSCOPY BASED ON A DIFFERENCE FREQUENCY GENERATOR

The experimental setup of our laser spectroscopic system is shown in Fig. 9. We mix two single-frequency signals with wavelengths $1027-1100\,\text{nm}$ and $1527-1600\,\text{nm}$ in a periodically poled nonlinear optical crystal. The signal is collimated and filtered by means of Si/Ge doublet, and split into the reference and probe beams. Astigmatic multi-pass gas cell (Aerodyne AMAC-76) is used to perform the trace-gas analysis at low pressures. One of the laser signals is generated by a commercial mode-hop-free widely tunable diode laser (Agilent 81600B) with a linewidth of $100\,\text{kHz}$, and amplified in a multistage polarization-maintaining (PM) erbium-doped fiber amplifier from $2\,\text{mW}$ to $40-50\,\text{mW}$.

Another signal is generated in a single-frequency widely tunable ytterbium-doped fiber amplifier. The laser has a fiber ring configuration with an intracavity high-finesse fiber ring resonator filter. The linewidth of the free-running laser is below $2\,\text{kHz}$ with occasional mode-hopping. The laser locked to the fiber ring resonator filter shows a linewidth increased to $50-100\,\text{kHz}$ as a result of low-frequency locking signal.[42] The signal of the ytterbium-doped fiber laser is amplified in a three-stage, core-pumped fiber amplifier to $170-190\,\text{mW}$. Low-gain, multi-stage amplifiers are used to prevent excessive growth of ASE around the gain peaks at $1030\,\text{nm}$ and $1530\,\text{nm}$, when the lasers are operated at a long-wavelength ends of the tuning range. No additional wavelength-controlled filters are used to filter ASE between the stages.

The amplified signals are wavelength multiplexed to the output pigtail. The z-axis polarized light from the output pigtail of the multiplexer is collimated by means of an anti-reflective coated achromatic lens with an effective focal length of $4\,mm$ and then it is focused on the (y,z) face of the periodically-poled KTP or KTA

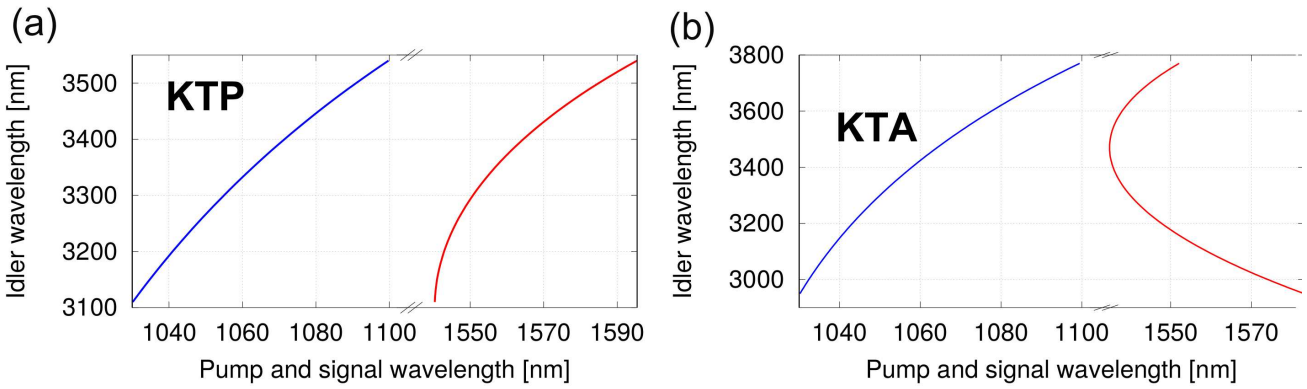

Figure 10. Phase matching condition for (a) KTP with a poling period of and 35.9 μm, and (b) KTA crystal with a poling period of 39.5 μm.

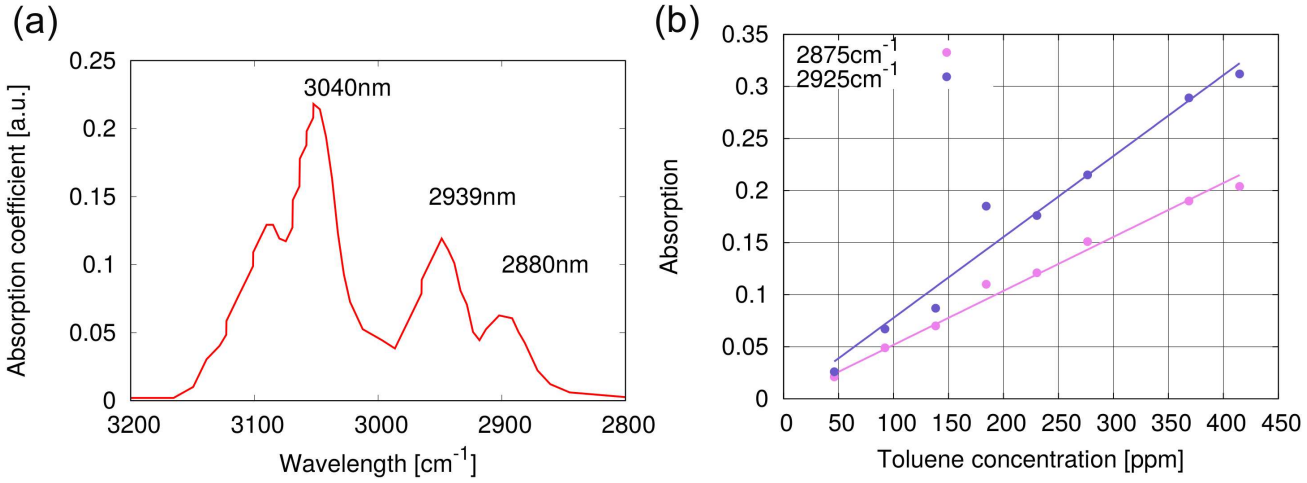

Figure 11. (a) IR absorption spectrum of toluene. (b) Absorption dependence on toluene concentration at two wavenumbers.

crystal using an anti-reflective coated achromatic doublet with a focal length of 30 mm. We used periodically poled nonlinear optical crystals 16.5 mm long and 1 mm thick with a length of the poled pattern of 15 mm. The difference frequency signal at the output of the crystal is collimated and filtered by an Si/Ge doublet and split by a pellicle beamsplitter into the reference and probe beams. The probe beam is coupled into the astigmatic multi-pass gas cell and directed to thermo-electrically cooled MCT detector (Hamamatsu C12495-211S). The reference signal is detected by a PbSe detector (Thorlabs PDA-20H).

The master oscillators are synchronously tuned to achieve the targeted mid-infrared frequency so that the phase-matching is maintained all the time The phase-matching condition is given by

$$\frac{2\pi}{\lambda_p} n_p - \frac{2\pi}{\lambda_s} n_s - \frac{2\pi}{\lambda_i} n_i = \frac{2\pi}{\Lambda}, \tag{11}$$

where Λ is the pattern period and $\lambda_{p,s,i}$ and $n_{p,s,i}$ are wavelengths and refractive indices of the pump, signal and idler, respectively. The refractive index is a function of the wavelength and can be expressed by Sellmeier formula, the coefficients of which are tabulated for KTP and KTA crystals.[43] Equation (11) is valid for plane waves with small deviations in wavelengths for Gaussian beams. The testing of the system was first performed for toluene with still unoptimized system. The absorption was measured as a function of concentration at atmospheric pressure and wavelengths close to two relatively week absorption peaks. A sensitivity of 10 ppm of toluene was achieved with a potential improvement by several orders of magnitude after system optimization (Fig. 11).

5. CONCLUSIONS

An Overview of laser absorption spectroscopy (LAS) techniques was given.o Requirements on coherent sources for panoramic mid-infrared LAS were formulated. Basic features of laser diodes, optical parametric oscillators and difference frequency generators were reviewed. Preliminary results for panoramic LAS system based on difference frequency mixing and operating in a spectral range of $2900 - 3800\,\mathrm{nm}$ were presented.

Acknowledgements

The work was supported by the Ministry of Education, Youth and Sports under Grant No. LD14112 in the frame of COST Action MP1204.

REFERENCES

[1] Hodgkinson, J. and Tatam, R. P., "Optical gas sensing: a review," *Measurement Science and Technology* **24**(1), 012004 (2013).

[2] Spearrin, R. M., Goldenstein, C. S., Schultz, I. A., Jeffries, J. B., and Hanson, R. K., "Simultaneous sensing of temperature, CO, and CO2 in a scramjet combustor using quantum cascade laser absorption spectroscopy," *Applied Physics B* **117**(2), 689–698 (2014).

[3] Frish, M. B., Wainner, R. T., Stafford-Evans, J., Green, B. D., Allen, M. G., Chancey, S., Rutherford, J., Midgley, G., and Wehnert, P., "Standoff sensing of natural gas leaks: Evolution of the remote methane leak detector (RMLD)," in [*Conference on Lasers and Electro-Optics/Quantum Electronics and Laser Science and Photonic Applications, Systems and Technologies*], *Conference on Lasers and Electro-Optics/Quantum Electronics and Laser Science and Photonic Applications, Systems and Technologies* , JThF3, Optical Society of America (2005).

[4] Parsons, M. T., Sydoryk, I., Lim, A., McIntyre, T. J., Tulip, J., Jäger, W., and McDonald, K., "Real-time monitoring of benzene, toluene, and p-xylene in a photoreaction chamber with a tunable mid-infrared laser and ultraviolet differential optical absorption spectroscopy," *Appl. Opt.* **50**(4), A90–A99 (2011).

[5] Kim, S., Klimecky, P., Jeffries, J. B., Jr, F. L. T., and Hanson, R. K., "In situ measurements of HCl during plasma etching of poly-silicon using a diode laser absorption sensor," *Measurement Science and Technology* **14**(9), 1662 (2003).

[6] Schaepkens, M., Martini, I., Sanjuan, E. A., Li, X., Oehrlein, G. S., Perry, W. L., and Anderson, H. M., "Gas-phase studies in inductively coupled fluorocarbon plasmas," *Journal of Vacuum Science & Technology A* **19**(6), 2946–2957 (2001).

[7] Wang, C. and Sahay, P., "Breath analysis using laser spectroscopic techniques: Breath biomarkers, spectral fingerprints, and detection limits," *Sensors (Basel, Switzerland)* **9**(10), 8230–8262 (2009).

[8] Bomse, D. S., Stanton, A. C., and Silver, J. A., "Frequency modulation and wavelength modulation spectroscopies:comparison of experimental methods using a lead-salt diode laser," *Appl. Opt.* **31**(6), 718–731 (1992).

[9] Hinkley, E. D., "High-resolution infrared spectroscopy with a tunable diode laser," *Applied Physics Letters* **16**(9), 351–354 (1970).

[10] Hinkley, E. D. and Kelley, P. L., "Detection of air pollutants with tunable diode lasers," *Science* **171**(3972), 635–639 (1971).

[11] Duffin, K., McGettrick, A. J., Johnstone, W., Stewart, G., and Moodie, D. G., "Tunable diode-laser spectroscopy with wavelength modulation: A calibration-free approach to the recovery of absolute gas absorption line shapes," *J. Lightwave Technol.* **25**(10), 3114–3125 (2007).

[12] Henningsen, J. and Simonsen, H., "Quantitative wavelength modulation spectroscopy with diode lasers," in [*Advanced Semiconductor Lasers and Their Applications*], *Advanced Semiconductor Lasers and Their Applications* , 25, Optical Society of America (1999).

[13] Henningsen, J. and Simonsen, H., "Quantitative wavelength-modulation spectroscopy without certified gas mixtures," *Applied Physics B* **70**(4), 627–633 (2000).

[14] Rieker, G. B., Jeffries, J. B., and Hanson, R. K., "Calibration-free wavelength-modulation spectroscopy for measurements of gas temperature and concentration in harsh environments," *Appl. Opt.* **48**(29), 5546–5560 (2009).

[15] Bjorklund, G. C., "Frequency-modulation spectroscopy: a new method for measuring weak absorptions and dispersions," *Opt. Lett.* **5**(1), 15–17 (1980).

[16] Janik, G. R., Carlisle, C. B., and Gallagher, T. F., "Two-tone frequency-modulation spectroscopy," *J. Opt. Soc. Am. B* **3**(8), 1070–1074 (1986).

[17] Cole, G. D., Zhang, W., Bjork, B. J., Follman, D., Heu, P., Deutsch, C., Sonderhouse, L., Robinson, J., Franz, C., Alexandrovski, A., Notcutt, M., Heckl, O. H., Ye, J., and Aspelmeyer, M., "High-performance near- and mid-infrared crystalline coatings," *Optica* **3**(6), 647–656 (2016).

[18] The VIRGO Collaboration, "The VIRGO large mirrors: a challenge for low loss coatings," *Classical and Quantum Gravity* **21**(5), S935 (2004).

[19] O'Keefe, A. and Deacon, D. A. G., "Cavity ring-down optical spectrometer for absorption measurements using pulsed laser sources," *Review of Scientific Instruments* **59**(12), 2544–2551 (1988).

[20] Meijer, G., Boogaarts, M. G., Jongma, R. T., Parker, D. H., and Wodtke, A. M., "Coherent cavity ring down spectroscopy," *Chemical Physics Letters* **217**(1), 112–116 (1994).

[21] O'Keefe, A., Scherer, J. J., and Paul, J. B., "cw Integrated cavity output spectroscopy," *Chemical Physics Letters* **307**(5–6), 343–349 (1999).

[22] Engeln, R., Berden, G., Peeters, R., and Meijer, G., "Cavity enhanced absorption and cavity enhanced magnetic rotation spectroscopy," *Review of Scientific Instruments* **69**(11), 3763–3769 (1998).

[23] Paul, J. B., Lapson, L., and Anderson, J. G., "Ultrasensitive absorption spectroscopy with a high-finesse optical cavity and off-axis alignment," *Appl. Opt.* **40**(27), 4904–4910 (2001).

[24] Maisons, G., Carbajo, P. G., Carras, M., and Romanini, D., "Optical-feedback cavity-enhanced absorption spectroscopy with a quantum cascade laser," *Opt. Lett.* **35**(21), 3607–3609 (2010).

[25] Gorrotxategi-Carbajo, P., Fasci, E., Ventrillard, I., Carras, M., Maisons, G., and Romanini, D., "Optical-feedback cavity-enhanced absorption spectroscopy with a quantum-cascade laser yields the lowest formaldehyde detection limit," *Applied Physics B* **110**(3), 309–314 (2013).

[26] Ye, J., Ma, L.-S., and Hall, J. L., "Ultrasensitive detections in atomic and molecular physics: demonstration in molecular overtone spectroscopy," *J. Opt. Soc. Am. B* **15**(1), 6–15 (1998).

[27] Schiller, S., "Spectrometry with frequency combs," *Opt. Lett.* **27**(9), 766–768 (2002).

[28] Coddington, I., Newbury, N., and Swann, W., "Dual-comb spectroscopy," *Optica* **3**(4), 414–426 (2016).

[29] Werle, P., "A review of recent advances in semiconductor laser based gas monitors," *Spectrochimica Acta Part A: Molecular and Biomolecular Spectroscopy* **54**(2), 197 – 236 (1998).

[30] Smid, R., Cizek, M., Mikel, B., and Cip, O., "Frequency noise suppression of a single mode laser with an unbalanced fiber interferometer for subnanometer interferometry," *Sensors* **15**(1), 1342 (2015).

[31] Wei, F., Yang, F., Zhang, X., Xu, D., Ding, M., Zhang, L., Chen, D., Cai, H., Fang, Z., and Xijia, G., "Subkilohertz linewidth reduction of a DFB diode laser using self-injection locking with a fiber Bragg grating Fabry-Perot cavity," *Opt. Express* **24**(15), 17406–17415 (2016).

[32] Li, C., Xu, S., Feng, Z., Xiao, Y., Mo, S., Yang, C., Zhang, W., Chen, D., and Yang, Z., "The ASE noise of a yb^{3+} -doped phosphate fiber single-frequency laser at 1083 nm," *Laser Physics Letters* **11**(2), 025104 (2014).

[33] Faist, J., Capasso, F., Sivco, D. L., Sirtori, C., Hutchinson, A. L., and Cho, A. Y., "Quantum cascade laser," *Science* **264**(5158), 553–556 (1994).

[34] Beck, M., Hofstetter, D., Aellen, T., Faist, J., Oesterle, U., Ilegems, M., Gini, E., and Melchior, H., "Continuous wave operation of a mid-infrared semiconductor laser at room temperature," *Science* **295**(5553), 301–305 (2002).

[35] Yang, R. Q., "Infrared laser based on intersubband transitions in quantum wells," *Superlattices and Microstructures* **17**(1), 77 – 83 (1995).

[36] Kim, M., Canedy, C. L., Bewley, W. W., Kim, C. S., Lindle, J. R., Abell, J., Vurgaftman, I., and Meyer, J. R., "Interband cascade laser emitting at λ=3.75μm in continuous wave above room temperature," *Applied Physics Letters* **92**(19) (2008).

[37] Yamada, M., Nada, N., Saitoh, M., and Watanabe, K., "First-order quasi-phase matched LiNbO3 waveguide periodically poled by applying an external field for efficient blue second?harmonic generation," *Applied Physics Letters* **62**(5), 435–436 (1993).

[38] Kefelian, F., Jiang, H., Lemonde, P., and Santarelli, G., "Ultralow-frequency-noise stabilization of a laser by locking to an optical fiber-delay line," *Opt. Lett.* **34**(7), 914–916 (2009).

[39] Jiang, H., Kéfélian, F., Lemonde, P., Clairon, A., and Santarelli, G., "An agile laser with ultra-low frequency noise and high sweep linearity," *Opt. Express* **18**(4), 3284–3297 (2010).

[40] Richter, D., Lancaster, D., Curl, R., and Tittel, F., "Tunable, fiber coupled spectrometer based on difference-frequency generation in periodically poled lithium niobate," in [*Advanced Solid State Lasers*], *Advanced Solid State Lasers* , WC5, Optical Society of America (1999).

[41] Richter, D., Lancaster, D. G., and Tittel, F. K., "Development of an automated diode-laser-based multi-component gas sensor," *Appl. Opt.* **39**(24), 4444–4450 (2000).

[42] Honzatko, P. and Baravets, Y., "Single-frequency fiber laser based on fiber ring resonator filter broadly tunable in a range 1030-1110nm," *To be published elsewhere* .

[43] Honzatko, P., Baravets, Y., Todorov, F., and Gladkov, P., "Comparison of widely tunable narrow-band CW MIR generators based on the difference frequency generation in KTP and KTA crystals," in [*Advanced Solid State Lasers*], *Advanced Solid State Lasers* , ATh2A.36, Optical Society of America (2014).